Fire Safety Journal 87 (2017) 18–24

Contents lists available at ScienceDirect

Fire Safety Journal

journal homepage: www.elsevier.com/locate/firesaf

Study of ignition and extinction of small-scale fires in experiments with an emulating gas burner

Frida Vermina Lundström[a,b,*], Peter B. Sunderland[c], James G. Quintiere[c], Patrick van Hees[a], John L. de Ris[d,1]

[a] Division of Fire Safety Engineering, Lund University, P.O. Box 118, SE-221 00 Lund, Sweden
[b] Danish Institute of Fire and Security Technology (DBI), Jernholmen 12, Hvidovre 2650, Denmark
[c] Department of Fire Protection Engineering, University of Maryland, 4356 Stadium Dr., College Park, MD 20742-3031, USA
[d] FM Global, USA

ARTICLE INFO

Keywords:
Combustion
Laminar diffusion flame
Heat flux gage

ABSTRACT

The objective of this study is to explore mechanisms for ignition and extinction for condensed-phase fuels via the use of a gas-fueled burner. Flames were generated with a porous 25 mm circular burner using mixtures of methane and propane with nitrogen. The procedure was to specify a set of mass fluxes of nitrogen-fuel mixture that corresponded to the flash- fire- and extinction points and for the minimum mass flux where steady burning was achieved. The results show an increase in the critical mass flux with a decreased heat of combustion. The data fall into two regimes depending on the mixture flow rate; one buoyancy-driven (Fr < 1) and one induced by momentum jet forces. The buoyancy-driven regime is geometrically consistent with the definitions of flash and fire points under natural convection conditions. The results for the momentum regime align reasonably with existing stagnant layer theory. Extinction theory is also suggested to give approximate results for the fire point. This argument is based on similar flame geometries for fire point and extinction and theoretical reasoning. An anchor point is proposed as the end point of ignition. Produced anchor point data result in a flammability diagram, below which quasi-steady burning occurs.

1. Introduction

Ignition is often referred to as the initiation of fire growth and is therefore an important parameter in the context of fire safety [1]. Various criteria are used for identifying when ignition and extinction for condensed-phase fuels occur. The most common for ignition is a critical surface temperature. For most liquid fuels the criterion is the flash or fire point. But for solids the critical surface temperature will vary depending on the decomposition kinetics. Computational Fluid Dynamics (CFD) modellers using complex solid phase kinetics typically require a minimum mass flux for ignition, which avoids modelling gas phase ignition processes [2,3]. The work herein examines this minimum (critical) mass flux, and an associated critical energy flux, as criteria for ignition and extinction.

We will describe the ignition event by three terms: Firstly, a *flash point* is defined as the minimum mass flux for which a premixed flame propagates from the spark ignitor towards the burner surface. It occurs as a premixed fuel-oxidizer mixture approaches the lower flammability limit (LFL) at the surface. Secondly, a *fire point* is defined as the minimum mass flux for which the flame is sustained for at least 5 s. A fire point occurs if the fuel-supply from the vaporizing liquid (or pyrolyzing solid) is enough for a diffusion flame to anchor at the fuel surface as the premixed flame approaches the surface of the fuel. The fire point begins at slightly above the LFL.

It is worth pointing out that the flash- and fire points are traditionally defined by critical temperatures of liquids and not by critical mass fluxes. A critical temperature of the fuel is often a satisfactory method for characterizing ignition in case of product screening [1], however a critical mass flux of volatiles was first proposed by Bamford et al.[4] as a more fundamental approach for modelling of ignition. This work takes the approach of using a critical mass flux and define ignition thereafter.

For a liquid the flash point and fire points are nearly the same compared to steady burning where the surface attains close to its boiling point which is much higher [5,6]. Thus, an *anchor point* is defined here as the minimum mass flux for which a flame is sustained over the entire burner surface. It is the condition of steady burning, and the state that a real fuel rapidly will approach after the fire point. In a

* Corresponding author at: Division of Fire Safety Engineering, Lund University, P.O. Box 118, SE-221 00 Lund, Sweden.
E-mail address: frida.vermina_lundstrom@brand.lth.se (F.V. Lundström).
[1] Retired.

http://dx.doi.org/10.1016/j.firesaf.2016.11.003
Received 30 March 2016; Received in revised form 3 October 2016; Accepted 20 November 2016

Nomenclature

α	Thermal Diffusivity
β	Thermal Expansion Coefficient
c_p	Heat Capacity at Constant Pressure
δ	Boundary Layer Thickness
D	Diameter
Fr	Froude Number
g	Acceleration of Gravity
h_c	Convective Heat Transfer Coefficient
Δh_c	Heat of Combustion
$\Delta h_{c,F}$	Heat of Combustion of Pure Fuel
Δh_{ox}	Heat of Combustion per Gram of Oxygen Consumed (13.1 kJ/g-O_2)
k	Conductivity
L	Latent Heat of Vaporization
$\dot{m}''$	Mass Flow Rate/Mass Flux
$\dot{m}''_F$	Mass Flow Rate of Pure Fuel
$\dot{m}''_{cr}$	Critical Mass Flux for Extinction
$\dot{m}''_{ig,LFL}$	Critical Mass Flux for a Flash
Nu_D	Nusselt Number
$\dot{q}''_{net}$	Net Heat Flux
ρ_{fuel}	Density of Fuel
r	Radius
Ra_D	Rayleigh Number
T_f	Flame Temperature
T_0	Initial Temperature
T_s	Fuel Vaporization Temperature (Burner Surface Temperature)
T_∞	Ambient Temperature
ΔT	Characteristic Temperature Difference
v	Velocity
υ	Kinematic Viscosity
X_r	Flame Radiation Fraction
Y_F	Fuel Mass Fraction in the Fuel Stream
Y_{ox}	Ambient Oxygen Mass Fraction

condensed-phase fuel the transition from the fire point to the anchor point is caused by a continuous feedback from the flame that increases the mass flux [7]. Finally, a threshold for *extinction* is defined as the mass flux where the flame extinguishes before 5 s has passed. The point of extinction, although disputed [8], is often argued to coincide with the firepoint.

An experimental assessment of a critical mass flux for condensed-phase fuels by conventional methods has been difficult due to the transient nature of the ignition (and extinction) process. As condensed-phase materials ignite they experience a rapid increase in mass loss, which is challenging to capture. The opposite is true for extinction. Several studies have determined the critical mass flux of various materials. Although refined methods exist [9], there are large discrepancies between data. The difficulties stem primarily from interpretation of the rate of mass loss, noise in the measurements, and, in some cases, phenomena involving intermittent flames and non-attached flames. Hence there is a need for developing experimental methodologies that can measure small changes in mass flux.

Motivated by the lack of consistency in experimentally determined mass flux data this work started with determining fuel flow rates at ignition and extinction with a newly developed apparatus called the burning rate emulator (BRE). BRE is inspired from previous experimental apparatuses. Corlett [10] initiated the use of gas burners for the study of steady burning pool fires, followed by Orloff and de Ris [11,12], Kim et al.[13], and Rasbash and Drysdale [7]. These studies show that condensed-phase burning may be investigated by experimentally separating gaseous reactions from the mass and energy balance at the surface. In mentioned studies quasi-steady burning was of primary focus, but the emphasis here is instead on ignition and extinction.

Existing stagnant layer theory readily explains how to gain mass flux data for the flash- and extinction points [14,15], however the mechanisms leading to the fire point are different from those of extinction. Despite this, Roberts and Quince [16] successfully used stagnant layer theory for the prediction of fire point. Results showed that flame temperatures could be accurately predicted by the assumptions of (i) negligible heat flux from the premixed flame to the liquid surface and (ii) negligible radiative heat flux from the established flame. Following their study, this work evaluates the applicability of extinction theory to fire point data, through phenomenological similarities and differences and through theoretical reasoning, following the boundary layer analysis by Quintiere [14,17].

2. Experimental design and procedure

The burning rate emulator is shown in Fig. 1. It is fed with a fuel and diluent which are monitored with Alicat gas mass flow controllers, ranging between 0 and 2 SLPM, before entering a mixing pipe. Well-mixed gases flow into a plenum through two supply tubes. Internally a ceramic honeycomb enables flow uniformity. Finally the mixture passes through an upward-facing circular porous copper plate with a diameter of 25 mm, replicating a solid sample with high porosity. Two combined K-type thermocouples and 1/8″ Medtherm heat flux gauges are mounted flush with the burner surface to measure surface temperature and heat flux close to the burner edge (r=8.25 mm) and centre (r=0 mm). The heat flux gauges have been calibrated by the supplier and then re-calibrated at the University of Maryland with the procedure detailed in NIST/BFRL Report of Test FR 4014 [18].

Initially different ignitors were used and the one giving the lowest mass flux at the flash and fire points was adopted. First, a vertical electrical arc gave a high temperature locally, but failed to cover the flammable zone. Secondly a pre-mixed fuel-air ignitor was used but the relatively high velocity blew away combustible gas. We found that the most robust ignitor for these experiments was a small propane diffusion flame ignitor. The ignitor was swept over the burner 2 mm above the burner surface, corresponding to the height of the Cleveland open cup test [19].

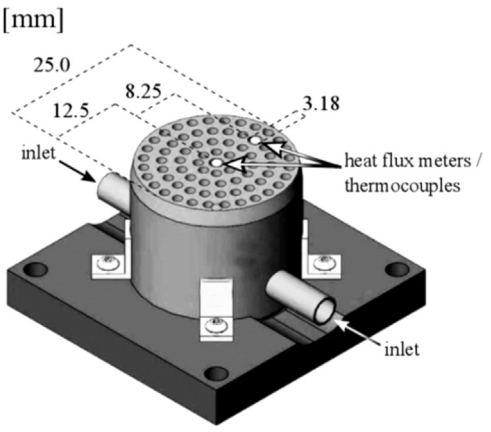

Fig. 1. Schematic of the BRE burner.

The experimental setup is located approximately one meter under a hood with low exhaust flow and the entire rig is protected from outer flow disturbances by a fine meshed net. Initial testing with incense streak lines proved this configuration satisfactory.

Fuels used are methane and propane which are diluted with nitrogen. An effective heat of combustion for each fuel/nitrogen mixture is found from

$$\Delta h_c = \frac{\dot{m}_F''}{\dot{m}''} \Delta h_{c,F}. \quad (1)$$

where $\dot{m}_F''$ and $\dot{m}''$ are mass flux of pure fuel and mixture respectively and $\Delta h_{c,F}$ is the heat of combustion of pure fuel.

A series of experiments were conducted to achieve flash, fire, anchor and extinction point data. The procedure was to specify a set of mass flow rates of nitrogen within the limits of the gas mass flow controllers. For each mass flow rate of nitrogen a corresponding fuel flow rate was obtained, for which the flash, fire point, anchor point and extinction point were recorded. Firstly, a flash point was determined by increasing the fuel mass flow rate to the point where a propagating flash from the ignitor towards the burner surface was seen. Local flashes, i.e., flames that do not propagate, or just partially propagate, were discarded, in consistency with the Cleveland open cup test [19]. The fuel flow was then increased until a fire point was reached. For the anchor point the mass flow rate of fuel was then increased up until a point where the entire surface of the burner was covered by the flame. Before any readings, the surface temperature was allowed to stabilize. Surface temperatures and heat fluxes were recorded in addition to the mass flow rate of the gases. Finally, an extinction point was obtained by stepwise decreasing the fuel flow rate to the point at which the flame extinguished.

In order to show applicability of BRE data to condensed-phase fuels, a comparison was made between BRE mass fluxes and mass fluxes for a number of plastics, irradiated with 50 kW/m^2 in the Cone Calorimeter. Cone experiments was performed in the Federal Aviation Administration (FAA) lab and analysed by Lyon [20]. It is assumed here that the critical mass flux is not dependent on the level of irradiance, as a flame fed with a given fuel supply ignites or extinguishes without any 'knowledge' of where the fuel came from. This is supported by the findings of Panagiotou and Quintiere, showing that the critical mass flux for ignition of four plastics is nearly constant for heat fluxes ranging between 20 and 50 kW/m^2[21].

A few experimental matters are noted with the use of the gas burner. Firstly, the BRE is not water cooled. Therefore the burner surface temperature was monitored to remain at ambient temperature (<30°C) for both flash and fire points. However, for an anchor or extinction point this was not possible; instead stabilized surface temperatures for those measurements were recorded. Secondly, propane, which is heavier than air, can gather at the burner surface when it is not diluted by nitrogen. Thus the first flash and fire point measurements are disregarded for propane; instead the second ignition is viewed as valid. Another point of apprehension is the velocity distribution over the burner surface. The BRE maintains a uniform velocity over the surface. On radiative ignition and on heating a liquid to determine its flash point, the condensed-phase has a fairly uniform velocity distribution. This is also true at the fire point before the impact of the premixed flame. But when a flame is established over a condensed-phase material, the burning achieves a heat flux distribution, and thus also a variable velocity over the surface. This is the case for the fire point after the impact of the premixed flame, and also for the anchor and extinction points. The velocity is greatest at the edge where the flame is closest to the surface. In this case, the BRE burner is imperfect. However, agreement between flame shapes in BRE to that of real materials, suggests that the initial burning velocity quickly adjusts to the diffusional flows of the flame [22].

3. Flow regime results

Lyon and Quintiere [20] have shown that the critical energy flux (the fuel flow rate multiplied by its heat of combustion) is constant over a range of materials (heat of combustions) at the flash and fire points, showing values of 21 ± 6 and 66 ± 17 kW/m^2 for the flash and fire point in the cone calorimeter. This is also partly true for BRE results, shown in Fig. 2(a), where the critical energy fluxes for flash, fire and extinction points are plotted.

Fig. 2(a) also shows that there is a regime where the statement of a constant critical energy flux doesn't hold. At low heats of combustion the critical energy flux increases rapidly with a decreasing heat of combustion. Experimental observations imply that burning is buoyancy-driven at low flow rates, whereas burning at high flow rates depend on momentum jet forces. This is supported by the flame not being attached to the burner surface at high mass fluxes. Theoretically the transition between the two regimes is explained by the Froude number ($Fr = v/\sqrt{gD}$; $v = \dot{m}''/\rho_{fuel}$) where Fr < 1 indicates buoyant flow and Fr > 1 is momentum-driven. At, and close to, Fr=1 there is a transitional behavior, where the flame is both buoyancy and momentum-driven.

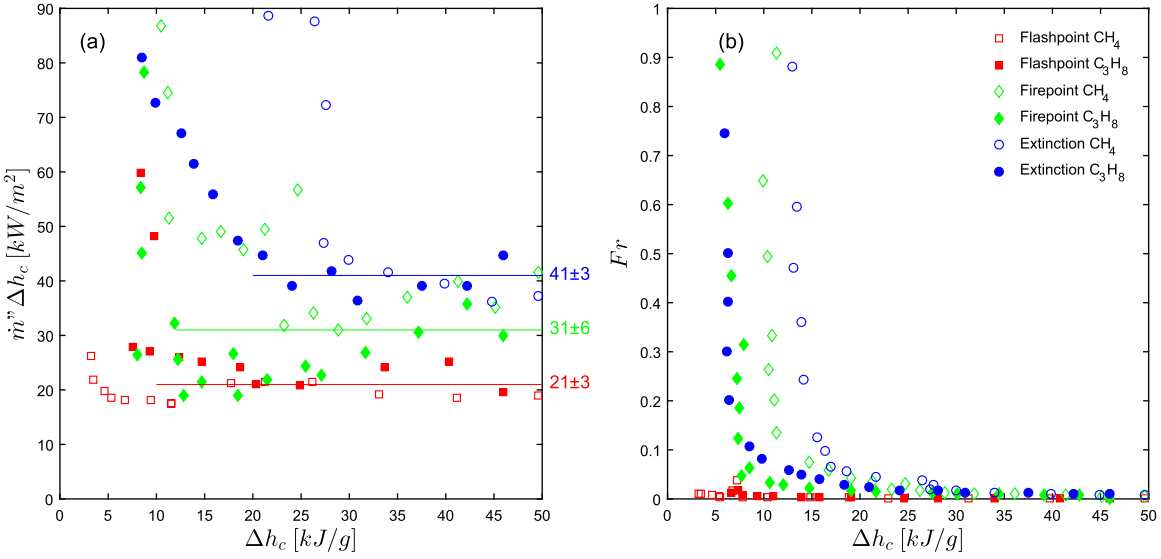

Fig. 2. Comparison of flash, fire and extinction points: (a) Critical energy flux, and; (b) Froude number.

Returning to Fig. 2(b), a rise in calculated *Fr* is initiated at Δh_c=5–10 kJ/g for the flash point and at Δh_c=5–15 kJ/g and Δh_c=5–20 kJ/g for the fire point and extinction respectively, where Fr approaches (flash point) or equals (fire point and extinction) unity. This approximately concurs with the visual determination of flame lift-off, occurring at Δh_c=10, 12, and 20 kJ/g for the flash, fire and extinction points respectively.

In the transient region, a flame with a methane/nitrogen mixture is sometimes extinguished due to a flame instability introduced when the supply velocity approaches the burning velocity of methane. Methane is also easily affected by outer disturbances. Because of this a few unrealistic methane results in the transient region have been discarded. After this consideration, averaged critical energy fluxes in the buoyant region are 21 ± 3, 31 ± 6, and 41 ± 3 kW/m^2 for flash- fire and extinction points respectively (or 21 ± 3, 35 ± 10, and 49 ± 17 kW/m^2 with transient methane results included). In other words, the BRE suggests that fire point and extinction are not identical and that a higher critical mass- or energy flux is seen when a flame is extinguished than at the fire point. The averages are shown for the buoyant regions as solid lines in Fig. 2(a).

4. Flash point

4.1. Flame appearance

In the BRE, as the ignitor flame reaches the burner rim, a blue flash propagates over the entire burner surface. The flame moves rapidly close to the surface before it extinguishes upon reaching the opposite side of the burner. With increasing flow velocity the flash no longer propagates along the burner surface. The premixed flame instead propagates through the flow field above the burner where the supply velocity of fuel matches the flame velocity. This produces a lifted flame.

4.2. Flash point theory

A stagnant layer one-dimensional model, previously developed by Quintiere [17] is used for evaluating experimental data. At the flash point, the mole fraction of vaporized fuel at the fuel surface is close to its LFL. The liquid fuel vapours are released at a constant rate and then diffuse and convect upwards. The highest fuel concentration is at the surface. A low burning rate is assumed, leading to following expression

$$\dot{m}''_{ig,LFL} \approx \frac{h_c}{\Delta h_c}(T_f - T_0). \quad (2)$$

In Eq. (2) h_c is the convective heat transfer coefficient, and Δh_c the effective heat of combustion for the fuel/nitrogen mixture. T_f and T_0 denote flame and initial temperatures. By assuming constant values for h_c, T_0 and T_f it is seen that $\dot{m}''_{ig,LFL}$ is a function of Δh_c. The reader is referred to Ref. [17] for a thorough derivation of the equation.

In stagnant layer analysis the convective heat transfer coefficient is approximated by $h_c = k/\delta$, where k is the thermal conductivity and δ is the thickness of the thermal boundary layer. Our approach is to utilize heat transfer correlations from literature to find the convective heat transfer coefficient. Gebhart derived a correlation for a hot plate facing up [23]

$$Nu_D = 0.43 + 0.60 Ra_D^{1/4}. \quad (3)$$

where Nu is the Nusselt number ($Nu_D \equiv h_c D/k$) and Ra is the Rayleigh number ($Ra_D \equiv g\beta\Delta T D^3/\alpha\nu$), evaluated at a film temperature. A complete list of terms is found in the nomenclature. For the calculation of the heat transfer coefficient we use gas properties from the SFPE Handbook [24], which results in $h_c = 6 W/m^2 K$ for the flash point. In the evaluation, T_0 is 298 K. The flame temperature T_f is taken as 1600 K for both the flash point and extinction, in line with the results of Maček and Williams amongst others [25,26]. The flame temperature is independent of fuel dilution since the mass stoichiometric air to fuel ratio is large.

4.3. Burning rate emulator results

In Fig. 3 flash point BRE results are presented along with experimental results for plastics in the Cone Calorimeter [20] and a theoretical solid line based on Eq. (2). The critical mass flux increases as the effective heat of combustion decreases. In other words, liquids and plastics (with relatively high Δh_c) exhibit lower mass flux values than charring materials (with relatively low Δh_c) at the flash point [20]. The minimum mass flux for flashing increases for materials with heats of combustion lower than 4–8 kJ/g, as is seen by both the theoretical solid trace and the experimental dots in Fig. 2. Below these values flashing is less likely.

Although Fig. 3 shows that BRE results match the magnitude and scatter for real plastics well, the theoretical description underestimates the results. Property assumptions is one reason for this discrepancy, especially the convective heat transfer coefficient has an impact on the critical mass flux, as seen in Eq. (2). A theoretical h_c of 12 W/m^{2}K would hit the experimental data. Another reason for the discrepancy is that the theory assumes a flash at the LFL. It is likely that this limit is not captured experimentally. At high mass flow rates the theory deviates from the experimental data. This is attributed to a theoretical assumption of a low burning rate assumed in Eq. (2).

5. Extinction

5.1. Flame appearance

Fig. 4 shows variations in flame shape with mass flow rate for extinction. The appearance is discussed below in terms of flame height, width and shape as well as colour, flame location and oscillating behavior.

Firstly, for all fuels, the flame height increases with increasing mass flux. At high mass fluxes the flame lifts off and the flame stand-off distance may be several mm. The lift-off is caused by the flame losing its stability close to the rim as a large excess of air is entrained at the flame base.

The width of the flame also increases with increasing mass flux up to the point where the flame lifts off from the burner surface. In the low mass flux zone (0–1.5 g/m^{2}s), indicative of a buoyancy dominated flow field, the flame is centred at a small portion of the burner. It is attached to the burner surface but not to the rim. The buoyant flame has a conical shape and a blue luminosity. It is anchored to the centre of the burner and flickers only at the last instant before it goes out. The buoyancy-driven flame is very close to the burner surface, which means that the flame loses much heat to the surface via conduction. If there is

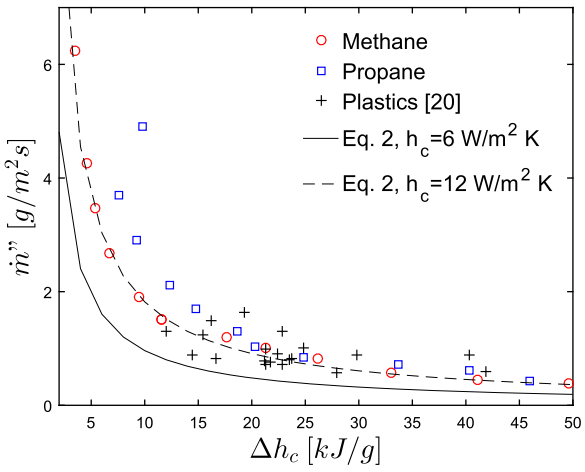

Fig. 3. Mass loss rate at the flash point.

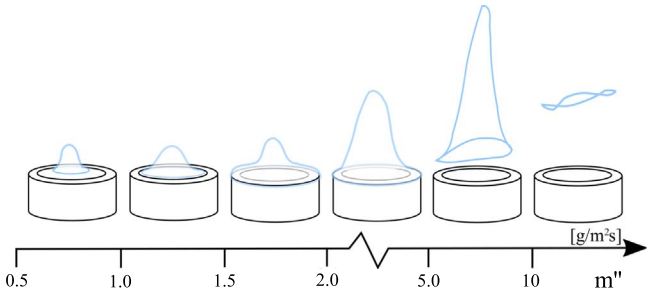

Fig. 4. Extinction behavior: Sketches of flame appearance at different mass fluxes. (For interpretation of the references to color in this figure, the reader is referred to the web version of this article).

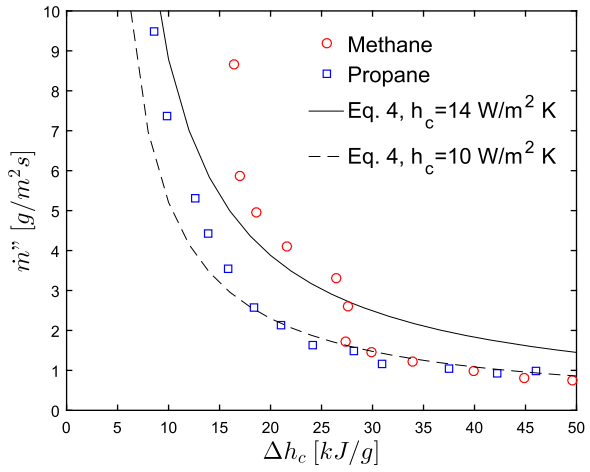

Fig. 5. Extinction behavior: critical mass flux.

not sufficient supply of fuel the flame is quenched by those heat losses. The flame at 1.5–2.0 g/m^2 s is attached to the burner rim. As the mass flux is slightly increased (2–5 g/m^2 s) the flame gets more robust against thermal quenching and a wider flame is visible. The flames are attached to the entire burner surface and oscillate in an axisymmetric fashion. The lifted flame, where the mass flux is 5–15 g/m^2 s, has moved inwards from the edge, just slightly. This may have to do with the flame compelling to stoichiometric conditions. The flame is cavernous with a non-luminous core and the flame stand-off distance may be several mm.

5.2. Extinction theory

Using stagnant layer theory, Quintiere and Rangwala [15] derived following equation for the critical mass flux at extinction

$$\dot{m}''_{cr}=\frac{\frac{h_c}{c_p}[Y_{ox}(1-X_r)\Delta h_{ox}-c_p(T_s-T_\infty)]}{Y_F\Delta h_c+c_p(T_s-T_\infty)-c_p(T_f-T_\infty)\left(1+\frac{\Delta h_c}{\Delta h_{ox}}\frac{Y_F}{Y_{ox}}\right)}. \quad (4)$$

where Y_{ox} is the oxygen mass fraction, X_r is the radiative fraction, Δh_{ox} is the heat of combustion per unit gram of oxygen consumed, c_p is the specific heat capacity, T_∞ is the ambient temperature, and Y_F is the fuel mass fraction. This equation is used for analysing extinction experiments. The theory will not be explained in this work. Eq. (4) is assumed to have the following values: Y_{ox}=0.233 because the test setup was well-ventilated, X_r=0 as the flames were blue, indicating low radiation, Δh_{ox}=13.1 kJ/g-O$_2$ [27], c_p=1 kJ/kgK [14], T_f=1600 K [25,26], and an assumed T_∞=298 K. The average surface temperature was measured to 400 K for both propane and methane at the point of extinction in a buoyant region and that is also the temperature that has been chosen as surface temperature for the theoretical line.

5.3. Burning rate emulator results

Extinction measurements are presented in Fig. 5 along with a solid line based on Eq. (4). The Froude number is plotted against the right-hand side y-axis, indicating a buoyant flow field when $\Delta h_c > 20 kJ/g$.

The theoretical description overestimates the results. This is likely due to sensitivity of the heat transfer coefficient. A heat transfer coefficient of h_c=14 W/m^{2}K is calculated from Eq. (3). Re-calculating with h_c=10 W/m^{2}K fits the experimental data in the buoyant region better. It should be noted that the approximate model used in this study relies on an accurate convective heat transfer correlation. Our approach has been to find the best correlation from literature that can deal with low Rayleigh numbers. Ra is associated with the boundary layer flow and when $Ra \rightarrow 0$ there is pure diffusion. Small adjustments of constants are common in heat transfer and may have a large impact on the end result.

6. Considerations of applying extinction theory to fire point data

6.1. Flame appearance

The appearance of a flame is an important characteristic when studying laminar diffusion flames, as it may give indications of the fundamental behavior depicting the appearance, e.g. the effects of air and gas movement. Flame colour, for instance, indicates radiative influence, but the colour also reveals where a fuel-rich core exists and where combustion takes place [10]. Another example is flame height which has been shown to correlate with mass flux at different burner geometries [28]. With this in mind, we propose consideration of extinction theory for fire point data. The BRE results namely suggest that the flame appearance for fire point is identical to that of extinction (refer Fig. 4). Flame heights and width are similar for similar mass fluxes. Also oscillating behavior, colour and flame location match the flame at extinction. In Fig. 6 example flames at fire point and extinction are presented to show the similarity. Analogous to extinction: At low mass fluxes the flame takes a conical shape and the flame does not necessarily cover the entire burner surface. At high mass fluxes the flame lifts off and the flame stand-off distance may be several mm; these measurements are not regarded to establish attached flames (i.e. not 'true' fire points) and are therefore mainly reported for completeness.

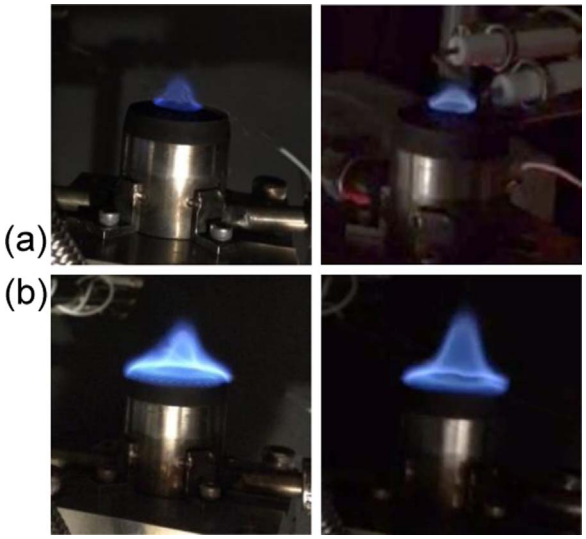

Fig. 6. Flame appearance: (a) fire point (LHS) and extinction flame (RHS) at $\dot{m}''$=0.70 g/(m^2 s) and (b) fire point (LHS) and extinction flame (RHS) at $\dot{m}''$=1.5 g/(m^2 s). (For interpretation of the references to color in this figure, the reader is referred to the web version of this article).

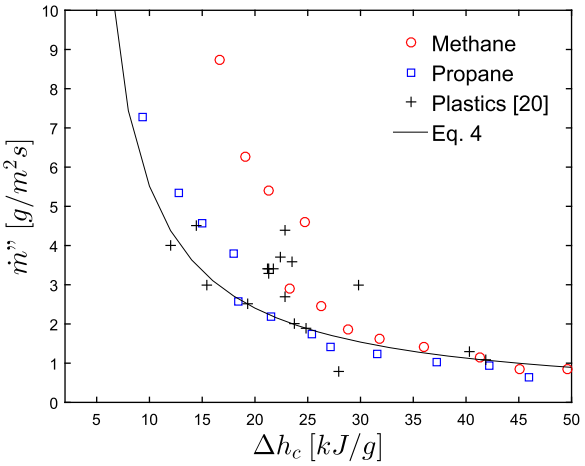

Fig. 7. Fire point behavior: Critical mass flux.

6.2. Burning rate emulator results

Fig. 7 presents the critical mass flux at the fire point based on various heats of combustion. Experimentally retrieved data for plastics matches the trend and the scattering for BRE results. Again, the transition from a buoyant to momentum driven regime is evaluated by the Froude number, shown by a right-hand side y-axis in Fig. 7. At, and close to, Fr=1 there is a transitional behavior, where the flame is both buoyancy and momentum-driven. This occurs at a heat of combustion of ~12 kJ/g. For Fr < 1 the flame is buoyant.

It seems reasonable to assume that a theoretical flame temperature of 1600 K may also be used for approximating fire point data. This has previously been verified by Roberts and Quince, who related the surface temperature at the fire point to that of the flame, finding limiting flame temperatures of 1530–1710 K [16]. Commonly the fire point is experimentally determined in terms of a surface temperature; however Spalding's theory does not suggest a critical surface temperature below which a flame cannot be sustained.

Despite similar flame appearances the validity of the theoretical application to fire point experiments is uncertain, due to the fact that the heat flow mechanisms determining extinction and fire point are different. Here we take use of an engineering approach, where a heat transfer coefficient for the fire point is estimated. The direction and magnitude of convective heat transfer can be discussed in terms of a characteristic temperature difference incorporated into the Rayleigh number. For example, the convective heat flow at the flash point goes from a hot burner surface to a colder ambient surrounding. For extinction, a characteristic temperature difference is instead found between a hot flame and the colder burner surface. We assume an intermediate value between these two cases for the fire point. This is because the fire point may be regarded as the transition between a hot surface (heated by a premixed flame) losing heat to the surrounding and an established flame losing heat to the burner surface. In other words, there is a change of both direction and magnitude of the convective flow at the fire point. An approximate value for the heat transfer coefficient of h_c=9 W/m^{2}K is obtained from Eq. (3). Data for real plastics [20], as well as BRE results, show encouraging agreement to the theory, when this approximation is applied.

It is worth noting that there is a larger heat loss from the flame to the burner surface at the fire point than at extinction, as the surface temperature at the fire point is lower (> 30°C). In future testing a water cooled burner will ensure a better comparison of the two phenomena.

7. Steady burning: anchor point

When ignition occurs for a material in a test apparatus with a pilot flame, the process begins with the flash point (premixed flame), then evolves to the fire point. However, for a liquid or solid fuel the feedback from the flame will increase the mass flux and drive the system from the fire point to full surface involvement. In this process the mass flux is increasing. We measure this end point as the "anchor point." For a liquid or non-charring solid the fuel can then attain steady burning.

The flame shape of the steady burning flame is similar to that of extinction for 2–5 g/m^{2}s (refer Fig. 4). The BRE allows us to define the anchor point where steady burning is initiated (i.e., the entire burner surface is fully involved in burning and the mass flux is fixed). The anchor point is determined by considering the average flame diameter vs. burner diameter. It is evident that the anchor point is not as easily obtained as the mixture flow rate is increased (jet regime). This is because the flame for high nitrogen flow rates initially is wide but is lifted from the burner. An anchor point is defined by flame attachment to the burner. Thus, for results in the jet regime the flame does not increase in diameter with increasing fuel rate, however the distance to the burner surface decreases.

The heat flux over the burner is estimated by using the two heat flux meters. Akita and Yumoto [29] have shown that the heat flux distribution over similar pool radii take an exponential form, where the heat flux to the edge is higher than that to the centre. An accurate description of the heat flux would place the measurements into such a distribution. Here the heat flux is approximated with a weighted average of an exponential distribution including the two heat flux meters

$$ln(q''_{net}) = \frac{\int_0^{12.5} 2\pi r\left[\frac{\ln(q''_{r=8.25mm}) - \ln(q''_{r=0mm})}{8.25} r + \ln(q''_{r=0mm})\right] dr}{\pi 12.5^2} \leftrightarrow q''_{net} = \frac{q''^{1.01}_{r=8.25mm}}{q''^{0.01}_{r=0mm}}. \quad (5)$$

where $\dot{q}''_{net}$ is the net heat flux, r is radius and $\dot{q}''_r$ is the heat flux at the locations of the heat flux meters. With this a heat of gasification ($L = \dot{q}''_{net}/\dot{m}''$) is calculated. This data was determined as the flow rate of diluent was gradually increased from the fire point to the maximum capacity of the flow meter. The convective heat transfer coefficient is taken as h_c=14W/m^2K as measured by Kim [30].

The gas burner is intended to emulate approximate generalized flammability results of liquids and solids. Fig. 8 presents a "flammability diagram", in terms of heat of gasification L and heat of combustion Δh_c. Below the regression line is a regime of steady burning. Above the line transient burning behavior may occur, such as ignition and extinction.

The slope of the line $L/\Delta h_c$ represents the fraction of energy released needed for continuation of steady burning. The inverted slope has previously been referred to as the combustibility ratio by Rasbash [31], or the heat release parameter (HRP) by Tewarson [32]. The

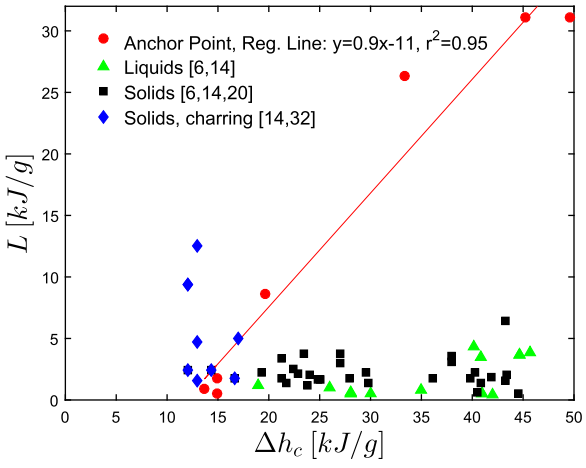

Fig. 8. Anchor point behavior: flammability diagram based on methane/nitrogen flow rates.

results show an approximate trend for liquids [6,14] and solids [6,14,20], whereas charring solids [14,32] (with low Δh_c) lie outside the domain of “steady burning”. This could be expected as char-forming materials do not burn without the support of external heating.

8. Conclusions

The BRE offers a simple and accurate way to emulate ignition and extinction conditions compared to standard tests for condensed-phase materials. While liquids and solids show rapid transitions at the moment of ignition, the BRE has the advantage of loading the fuel gas at a specific rate irrespective of the heat flux exposed onto the surface. As such, it has an additional degree of freedom to examine the mechanisms leading to ignition/extinction. By slowly increasing the fuel flow rate the BRE readily demonstrates the flame appearance, first at the flash point that with increasing fuel flow rate is followed by a fire point. At the fire point it is shown that a flame does not necessarily cover the entire fuel surface area in order to sustain. By increasing the fuel flow rate even further, an anchor point is proposed as the end point of the ignition phenomenon (or starting point of steady burning).

The critical mass flux criterion used for ignition and extinction is not a constant, but changes with the effective heat of combustion of the fuel. The data fall into two regimes depending on the flow rate of the mixture; one buoyancy-driven (Fr < 1) and one induced by momentum jet forces. The former is geometrically consistent with the stated definitions of flash- and fire points at natural convection, while the latter, although aligning with the theory presented, is driven by momentum forces. Lyon and Quintiere [20] has shown that the critical energy flux (the fuel flow rate multiplied by its heat of combustion) is constant over a range of materials (heats of combustion) at the flash and fire point. BRE results show that this is true in a buoyant region, but in the momentum jet region the critical energy flux varies with the heat of combustion.

Stagnant layer theory is suggested to approximately predict fire point data. The fore laid argument is based on the similar flame geometries exhibited at the fire point and point of extinction. However, the heat flow mechanisms leading up to the occurrence of a fire point are different from the heat transfer at extinction. Unlike extinction, there is a change of both direction and magnitude of the convective flow at the fire point. It is proposed that this may be accounted for through modification of the convective heat transfer coefficient.

Conclusively, BRE results match those of real condensed-phase fuels. The BRE's main advantage is that the gas flow (emulating pyrolysates or vapours) is independent of the heating source. As such it may be a support to better define the limiting conditions at ignition and extinction.

Conflict of interest

There are no, to the authors known, conflicts of interest in the completion of this work.

Acknowledgements and funding

The authors are truly grateful to dr. Haiqing Guo for discussions and assistance in the lab. The authors are also grateful to NASA for funding the development of the burner, under Grant no. NNX10AD98G. This study is part of FIRETOOLS which is a collaborate project between Lund University and the Danish Institute of Fire and Security Technology, funded by the European Union's Seventh Framework Programme under Grant no. 316991.

References

[1] D.D. Drysdale, An Introduction to Fire Dynamics, 2nd ed., John Wiley & Sons, Chichester, 1999, p. 193.
[2] S.I. Stoliarov, I.T. Leventon, R.E. Lyon, Two-dimensional model of burning for pyrolyzable solids, Fire Mater. 38 (3) (2014) 391–408.
[3] C.W. Lautenberger, A Generalized Pyrolysis Model for Combustible Solids(Ph.D. Dissertation), University of California, Berkeley, 2007.
[4] CH. Bamford, J. Crank, DH. Malan, H. Wilson, The Combustion of Wood. Part I, in: Mathemathical Proceedings of the Cambridge Philosophical Society, vol. 42(2), 1946, pp.166–182.
[5] D.D. Drysdale, Ignition of liquids, in: M.J. Hurley (Ed.)SFPE Handbook Fire Protection Engineering5th ed., Springer, New York, 2015, p. 568.
[6] F.W. Mowrer, Fundamentals of the fire hazards of materials, in: C.A. Harper (Ed.) Handbook of Building Materials for Fire Protection, McGraw-Hill Book Co, New York, 2004, p. 1.25.
[7] D.D. Rasbash, D.D. Drysdale, Theory of fire and fire processes, Fire Mater. 7 (2) (1983) 79–88.
[8] J. Dai, M.A. Delichatsios, L. Yang, et al., Piloted ignition and extinction for solid fuels, Proc. Combust. Inst. 34 (2014) 2487–2495.
[9] M.M. Khan, J.L. de Ris, Operator independent ignition measurements, Fire Saf. Sci. 8 (2005) 163–174.
[10] R.C. Corlett, Gas fires with pool-Like boundary conditions, Combust. Flame 12 (3) (1968) 19–32.
[11] J.L. De Ris, L. Orloff, A dimensionless correlation of pool burning data, Combust. Flame 18 (3) (1972) 381–388.
[12] J.L. De Ris, L. Orloff, The role of buoyancy direction and radiation in turbulent diffusion flames on surfaces, Symp. (Int.) Combust. 15 (1975) 175–182.
[13] J.S. Kim, J.L. De Ris, F.W. Kroesser, Laminar free-convective burning of fuel surfaces, Symp. (Int.) Combust. 13 (1971) 949–961.
[14] J.G. Quintiere, Fundamentals of Fire Phenomena, John Wiley & Sons, Chichester, 2006, pp. 227–296.
[15] J.G. Quintiere, A.S. Rangwala, A theory for flame extinction based on flame temperature, Fire Mater. 28 (5) (2004) 387–402.
[16] A.F. Roberts, B.W. Quince, A limiting condition for the burning of flammable liquids, Combust. Flame 251 (2) (1973) 245–251.
[17] J.G. Quintiere, A theoretical basis for flammability properties, Fire Mater. 30 (3) (2006) 175–214.
[18] WM. Pitts, JR. Lawson, JR. Shields, Report of Test FR 4014: NIST/BFRL Calibration System for Heat-Flux Gages, NIST, Gaitherburg, 2001.
[19] American Society for Testing Materials, Standard Test Method for Flash and Fire Points by Cleveland Open Cup Tester. ASTM D92-12b, ASTM, Philadelphia, 2010.
[20] R. Lyon, J.G. Quintiere, Criteria for piloted ignition of combustible solids, Combust. Flame 151 (4) (2007) 551–559.
[21] J. Panagiotou, JG. Quintiere, Generalizing Flammability of Materials, in: Proceeding of the Interflam 2004, 10th International Fire Science and Engineering Conference, Greenwich, 2004, pp. 895–905.
[22] Y. Zhang, M. Kim, P.B. Sunderland, J.G. Quintiere, J.L. de Ris, A burner to emulate condensed phase fuels, Exp. Therm. Fluid Sci. 73 (5) (2016) 87–93.
[23] B. Gebhart, Heat Transfer, 2nd ed., McGraw-Hill Book Co, New York, 1971, pp. 371–372.
[24] Appendix 2: Thermophysical property data, in: M.J. Hurley et al. (Ed.), SFPE Handbook Fire Protection Engineering. 5th ed. New York: Springer, 2015, p. 3427.
[25] A. Maček, Flammability Limits: Thermodynamics and Kinetics, National Bureau of Standards, Center for Fire Research, Washington DC, 1976 (Final report no. PB-254180; NBSIR-76-1076).
[26] F.A. Williams, A review on flame extinction, Fire Saf. J. 3 (3) (1981) 163–175.
[27] M.L. Janssens, Measuring rate of heat release by oxygen consumption, Fire Technol. 27 (3) (1991) 234–249.
[28] F.G. Roper, The prediction of laminar jet diffusion flame sizes: Part I. Theoretical model, Combust. Flame 29 (1977) 219–226.
[29] K. Akita, T. Yumoto, Heat transfer in small pools and rates of burning of liquid methanol, Proc. Combust. Inst. 10 (1) (1965) 943–948.
[30] H. Kim, Procedures to Obtain Accurate Measurement from a Gas Fuelled Burner (Ms. Thesis), University of Maryland, College Park, 2014.
[31] DJ. Rasbash, Theory in the evaluation of fire properties of combustible materials, in: Proceedings of the 5th International Fire Protection Seminarium, Karlsruhepp, 1976, pp. 113–130.
[32] A. Tewarson, Generation of heat and chemical compounds in fire, in: P. DiNenno (Ed.)3th ed., SFPE Handbook Fire Protection Engineering 3–161, Springer, New York, 2002, pp. 3–82.